

Emergent Anisotropy and Flow Alignment in Viscous Rock

H-B Mühlhaus ^(1,2), L.Moresi ⁽³⁾, M. Cada ⁽⁴⁾,

(1,2) The University of Queensland, St Lucia, QLD 4072, Australia (e: mail: muhlhaus@quakes.ug.edu.au; phone +61 7 3365 4783; mobile: +61 403 390 966) & CSIRO Division of Exploration and Mining, 26 Dick Perry Ave., Kensington WA 6051, Australia (3) School of Mathematical Sciences, Monash University, PO Box 28M, Clayton, Victoria 3800, Australia (e-mail; louis.moresi@sci.monash.edu.au; phone:)
(4) Ludwig Maximilians Universität, Theresienstr. 41, 80333 Munich (miro.cada@addcom.de)

Abstract

A novel class of nonlinear, visco-elastic rheologies has recently been developed by Mühlhaus et al ([1,2]; see¹ for preprints). The theory has originally been developed for the simulation of large deformation processes including folding and kinking in multi-layered visco-elastic rock. The orientation of the layer surfaces or slip planes in the context of crystallographic slip is determined by the normal vector-the so-called director-of these surfaces. Here the model [1,2] is generalized to include thermal effects; it is shown that in 2D steady states the director is given by the gradient of the flow potential. The model is applied to anisotropic simple shear where the directors are initially parallel to the shear direction. The relative effects of textural hardening and thermal softening are demonstrated. Turning to natural convection we compare the time evolution and approximately steady states of isotropic and anisotropic convection for a Rayleigh number $Ra = 5.64 \times 10^5$. The isotropic case has a simple steady state solution, whereas the orthotropic convection model produces a continuously evolving patterning in the core of the convection cell, which makes only a near-steady condition possible.

¹⁾ <http://www.ned.dem.csiro.au/research/solidmech/Publications/>.

Introduction

During the past decade, geoscientists have come to appreciate the often-powerful role played by computer simulations as a tool to enhance our understanding of geological processes. While early simulations were often based on rheologies and computer packages from the engineering world, there is an increasing awareness that these methods are only suited for a limited number of geological problems.

Computer models must be constrained by observational data. In the case of studies of the Earth's interior, analysis of seismic observations has provided the principle information. In particular, seismic tomography is yielding ever-improved estimates of seismic wave velocities and anisotropy, which can be interpreted as a filtered snapshot of density and instantaneous flow pattern. There is, however, no time information on mantle

flow in the seismic data so the emergence of plate tectonics and material anisotropy must be deduced from other means. Computer simulations of these phenomena can in principle provide such a means. However a numerical simulation model for mantle convection and emergence of plate tectonics, which simulates the development of anisotropic texture of the lithosphere and mantle, is a difficult modelling exercise, requiring a sophisticated mix of developments of constitutive relationships and of numerical methodology. In this context, the seismic tomography derived anisotropy models of the earth (eg. Debayle & Kennett, [6]) represent an important constraint on present day flow patterns. The emergent anisotropy predicted in numerical simulations would improve interpretation of seismic tomography derived anisotropy models in terms of flow patterns and their evolution.

The direct simulation of anisotropic mantle flow has been a very specialized area with very few publications since the original paper of Christensen [3]. In general it has instead been assumed that the instantaneous flow patterns predicted by convection simulations can be mapped immediately to seismic anisotropy. However, the results of Simons et al [9] and many others show the observations to be far more advanced than this simplistic modeling assumption. Recent work by Parmentier and coworkers (Fischer et al[8]; Fouch et al [7]) is considerably more sophisticated, but does not treat the director as a distinct internal material variable. Advanced models should include feedback processes between large-scale flow, director mis-alignment and the drive towards flow alignment.

A step in this direction in the context of folding was described by Mühlhaus et al [1,2]. The present paper represents a continuation of this work; the rheology is refined to include temperature dependent parameters. The performance of the model is illustrated in finite element simulations of anisotropic simple shear and anisotropic natural convection.

Specific Viscous and Visco-Elastic Constitutive Relations

We consider a locally transverse-isotropic, viscous material. The transverse-isotropy may represent an alternating sequence of hard and soft materials or a superposition of layers of one and the same material, which are weakly bonded along their interfaces. Another important realization is crystallographic slip planes. The orientation of the anisotropy is characterized by a so called director which in the case of a layered material or crystallographic slip is oriented normal to the layer or slip surface respectively. The term ‘director’ is adopted from the physics of liquid crystals (de Gennes and Prost [5]). We designate normal shear viscosity as η and η_s is the shear viscosity measured in simple, layer parallel shear.

In the following simple model for a layered viscous material we correct the isotropic part $2\eta D'_{ij}$ of the model by means of the Λ tensor (Mühlhaus et al 2002 [1],[2]) to consider the mechanical effect of the layering; thus

$$\sigma_{ij} = 2\eta D'_{ij} - 2(\eta - \eta_s)\Lambda_{ijlm}D'_{lm} - p\delta_{ij} \quad (1)$$

where a prime designates the deviator of the respective quantity, p is the pressure, D_{ij} is the stretching, σ_{ij} is the Cauchy or true stress and

$$\Lambda_{ijkl} = \left(\frac{1}{2}(n_i n_k \delta_{lj} + n_j n_k \delta_{il} + n_i n_l \delta_{kj} + n_j n_l \delta_{ik}) - 2n_i n_j n_k n_l\right). \quad (2)$$

In (1) and (2) the vector n_i is the unit orientation vector of the director N_i . In the present applications we assume that the director transforms as a material surface element; using a standard result of continuum mechanics we find:

$$N_{i,t} + v_k N_{i,k} = -v_{k,i} N_k \quad (3)$$

where v_i is the velocity vector. The left hand side of (3) is the material time derivative of the director. For steady states the partial time derivative vanishes and (3) maybe re-written as:

$$v_k (N_{i,k} - N_{k,i}) = -(v_k N_k)_{,i} \quad (4)$$

In 2D it is plausible that the planes of anisotropy or slip planes are aligned with the velocity vectors in steady states, which is equivalent to normality of the directors to the velocity vectors. If normality holds then the right hand side of (4) vanishes. A solution $\mathbf{N} \perp \mathbf{v}$ exist if the left hand side vanishes as well. To show this we remember that for incompressible flow the velocity vectors can be derived from the rotational derivative of a vectorial (3D) or scalar (2D) potential. The gradient of this potential is obviously orthogonal to the velocity vectors and since the gradient of a scalar potential is also irrotational the right hand side of (4) vanishes. Hence, in steady states a solution for the directors exists such that the directors are point-wise orthogonal to the velocities. In this case the directors do not need to be included explicitly as independent variables, which simplifies the formulation considerably. The model equations are implemented into the finite element codes FASTFLO (<http://www.cmis.csiro.au/Fastflo/>) and Ellipsis (<http://www.ned.dem.csiro.au/research/solidMech/Codes.html#ELLIPSIS>) and the results presented are applications of those codes.

Simple Shear

We consider a semi-infinite layer parallel to x_1 with the thickness h . At $x_2=h$ we apply a constant shear stress τ ; also at $x_2=h$ we assume that the temperature is kept constant and $v_2=0$. At $x_2=0$ we assume that the velocities and the thermal gradient vanishes. At time $t=0$ the directors are assumed parallel to x_1 , i.e. the layering is initially orthogonal to the surface of the shear layer. We have considered two cases, namely simple shear with and without temperature dependence ($\sim \exp(Q/RT)$) of the viscosity. In both calculations we assume that $\eta/\eta_s = 10$. In the case of temperature independence we can use the following results to test the numerical solution: if the layers are orthogonal or parallel to the shear layer we must have $D_{12} = \tau/\eta_s$; if the layers have rotated by $\pi/4$ then $D_{12} = \tau/\eta$. The relevant dimensionless numbers are the Peclet number Pe (=process time/thermal diffusion time; process time is $h/(\text{ref. shear speed})$) and the dissipation number Di . In the dimensionless heat equation $1/Pe$ is the coefficient of the thermal diffusion term and Di is the coefficient of the mechanical dissipation. See e.g. Christensen [4] for details. In Figure 1, v_{\max} is the shear velocity at $x_2=h$ and T_{\max} is the temperature at $x_2=0$. In fig. 1 v_{\max} drops from 10 to 1 at $\Delta=1$ where the directors have rotated by $\pi/4$. For temperature dependent viscosity the textural hardening is counteracted by thermal softening; i.e. v_{\max} levels out and subsequently increase again after a director rotation of approximately $\pi/8$. The normal strain rates depend on the normal stress and the shear stress in anisotropic simple shear; hence the coupling between the shear stress and the normal stress ($\sigma_{22}/(\sigma_{12} = \tau)$) in Figure 1.

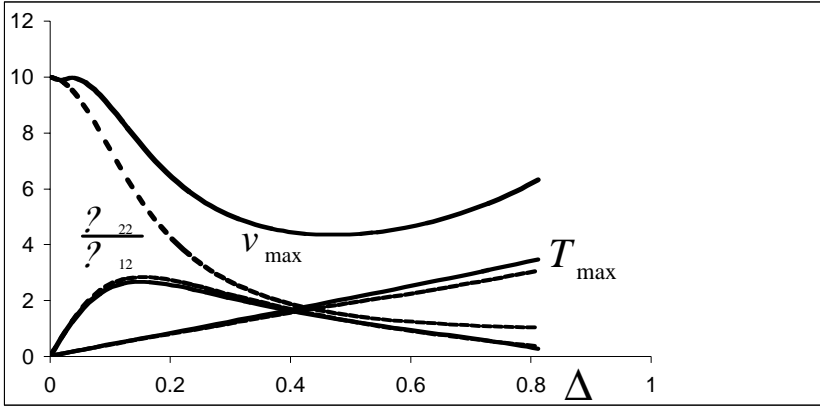


Figure 1: Simple shear of a layer of constant thickness h . The details of the boundary conditions are described in the text above. Constant viscosity simulations: broken line; temperature dependent viscosity: solid line. $Pe= 8400$ (i.e. thermal diffusion is unimportant) and $Di=0.9$. Δ is the shear displacement at $x_2=h$.

Anisotropic vs. Isotropic Convection

We consider a standard bottom heated convection box. On all boundaries we assume that the normal velocities are zero; on the top and bottom boundaries the temperature is kept fixed and on the sides the thermal gradient vanish. In each case we assume a Rayleigh number of $Ra=5.64 \times 10^5$ and $\eta/\eta_s = 10$. In the definition of the Rayleigh number for anisotropic viscous materials we follow Christensen [3] and define:

$$Ra = \frac{2\alpha\rho_0^2 c_p g \Delta T H^3}{D(\eta + \eta_s)} \quad (5)$$

The global characteristics represented in the figure 2 are the root mean square of the nodal point velocities and the Nusselt number, which in 2D for an box of aspect ratio 1 with zero normal velocities across the box surfaces is defined as:

$$Nu = 1 - \int_{-L/2}^{L/2} \frac{1}{2} (T_{,2}(x_1, \frac{1}{2}) + T_{,2}(x_1, -\frac{1}{2})) dx_1 \quad (6)$$

where T is the convective temperature. In the case of anisotropic convection, flow is concentrating around the cell boundaries encircling a more or less stagnant core. The simulations are based on 32×32 and 64×64 square meshes of bilinear quadrilateral. The momentum, heat and director equations are solved sequentially. Advection terms do not appear explicitly in the numerical formulation because of the Lagrangian nature of history information in ELLIPSIS. The initial overshoot and the subsequent drop of the parameters in Figure 2 is because the simulation was initiated at the most unstable state possible, the non-convecting ground state. The system passes through a variety of configuration until it

finally settles to the steady states shown in Figure 2. In the anisotropic case, this is a near-steady state in rms velocity and Nusselt number, but the alignment patterning in the core of the convection cell continues to evolve slowly, producing small fluctuations. In this final state, the boundary layers are well aligned with the flow, but strain-rate gradients towards the stagnant core of the cell “freeze” in a highly complicated pattern of orientation, which is nearly isotropic at the resolution of the mesh. Note the additional resolution needed in the orthotropic case — although the pattern of evolution of Nusselt number and rms velocity is qualitatively similar, only the final state is quantitatively comparable.

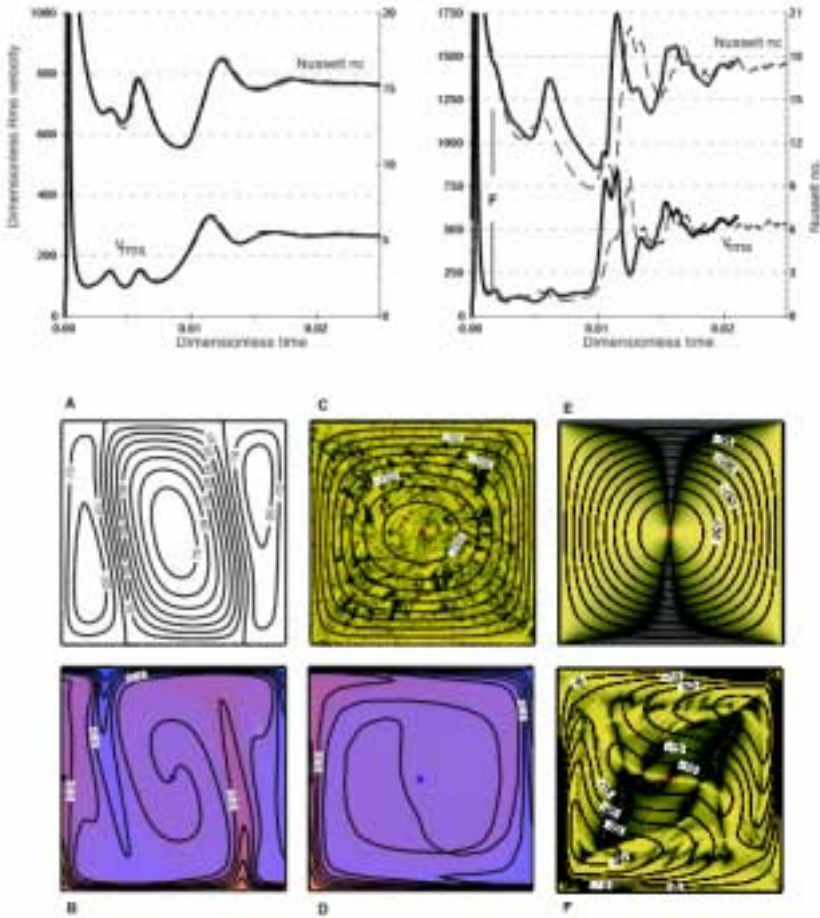


Figure 2. Time dependent Convection. $Ra=5.6 \times 10^5$. Time series plots of velocity and Nusselt number isotropic convection (top left) and anisotropic convection, $\eta / \eta_s = 10$ (top right). Dashed lines are the results of the 32x32 element simulations. The isotropic steady state stream function (A) and temperature field (B) are compared with the anisotropic quasi-steady state (C,D respectively). E,

F show stream function and flow alignment for the anisotropic case at times 0 (E) and 0.0009 (F). Alignment is computed by $\mathbf{n} \times \mathbf{v} / |\mathbf{v}|$ with misalignment indicated by dark regions.

References

- [1] H-B Mühlhaus, Dufour, F, Moresi, L, Hobbs, BE (2002) *A director theory for viscoelastic folding instabilities in multilayered rock*. Int. J. Solids and Structures. Vol. **39**; 3675-3691
- [2] H-B Mühlhaus, L.N Moresi, B. Hobbs, and F. Dufour (2002) *Large Amplitude Folding in Finely Layered Viscoelastic Rock Structures*, In the press PAGEOPH, To appear: 2002
- [3] U.C. Christensen (1987) *Some geodynamical effects of anisotropic viscosity*; Geophys.J.R.astr. Soc. **91**;711-736
- [4] U.C. Christensen (1984) *Convection with pressure and temperature dependent rheology*; Geophys. J.R. astr. Soc. **77**; 343-384
- [5] De Gennes, P.G. and Prost J. 1995 *The physics of liquid crystals*, 2nd edition, Clarendon Press, Oxford.
- [6] Debayle, E and BLN Kennett (2000) *Anisotropy in the Australian upper mantle from Love and Rayleigh waveform inversion*. Earth and Planetary Science Letters, **184**, 339-351.
- [7] Fouch, MJ; Fischer, KM; Parmentier, EM; Wysession, ME and Clarke, TJ (1997) *Shear wave splitting, continental roots, and patterns of mantle flow*, MIT-Harvard workshop on continental roots, Harvard, MA1997.
- [8] Fischer KM, Parmentier EM, Stine AR, Wolf ER (2000) *Modeling anisotropy and plate-driven flow in the Tonga subduction zone back arc*. J. Gophys. Res.-Solid Earth 105 (B7): 16181-16191
- [9] Simons, FJ; van der Hilst, RD; Montagner, J-P and Zielhuis, A (2002) *Multimode Rayleigh wave inversion for heterogeneity and azimuthal anisotropy of the Australian upper mantle* In Press Geophysical J. Int. preprint: <http://quake.mit.edu/~fjsimons/azimuthal.html>